J Physiol 595.2 (2017) pp 583–598

JPn Neuroscience
The Journal of Physiology

A novel enteric neuron–glia coculture system reveals the role of glia in neuronal development

Catherine Le Berre-Scoul, Julien Chevalier, Elena Oleynikova, François Cossais, Sophie Talon, Michel Neunlist and Hélène Boudin

INSERM UMR 913, IMAD, University of Nantes, France

Key points

- Unlike astrocytes in the brain, the potential role of enteric glial cells (EGCs) in the formation of the enteric neuronal circuit is currently unknown.
- To examine the role of EGCs in the formation of the neuronal network, we developed a novel neuron-enriched culture model from embryonic rat intestine grown in indirect coculture with EGCs.
- We found that EGCs shape axonal complexity and synapse density in enteric neurons, through purinergic- and glial cell line-derived neurotrophic factor-dependent pathways.
- Using a novel and valuable culture model to study enteric neuron–glia interactions, our study identified EGCs as a key cellular actor regulating neuronal network maturation.

Abstract In the nervous system, the formation of neuronal circuitry results from a complex and coordinated action of intrinsic and extrinsic factors. In the CNS, extrinsic mediators derived from astrocytes have been shown to play a key role in neuronal maturation, including dendritic shaping, axon guidance and synaptogenesis. In the enteric nervous system (ENS), the potential role of enteric glial cells (EGCs) in the maturation of developing enteric neuronal circuit is currently unknown. A major obstacle in addressing this question is the difficulty in obtaining a valuable experimental model in which enteric neurons could be isolated and maintained without EGCs. We adapted a cell culture method previously developed for CNS neurons to establish a neuron-enriched primary culture from embryonic rat intestine which was cultured in indirect coculture with EGCs. We demonstrated that enteric neurons grown in such conditions showed several structural, phenotypic and functional hallmarks of proper development and maturation. However, when neurons were grown without EGCs, the complexity of the axonal arbour and the density of synapses were markedly reduced, suggesting that glial-derived factors contribute strongly to the formation of the neuronal circuitry. We found that these effects played by EGCs were mediated in part through purinergic $P2Y_1$ receptor- and glial cell line-derived neurotrophic factor-dependent pathways. Using a novel and valuable culture model to study enteric neuron–glia interactions, our study identified EGCs as a key cellular actor required for neuronal network maturation.

(Received 4 December 2015; accepted after revision 7 July 2016; first published online 20 July 2016)
Corresponding author H. Boudin: INSERM UMR913, University of Nantes, 1, rue Gaston Veil, 44035 Nantes, France. Email: helene.boudin@univ-nantes.fr

Abbreviations AraC, 1-β-D-arabinofuranosylcytosine; BzATP, 2′(3′)-*O*-(4-benzoylbenzoyl)-ATP; ChAT, choline acetyltransferase; DIV, days *in vitro*; DMEM, Dulbecco's modified Eagle medium; DMPP, dimethylphenylpiperazinium; EGC, enteric glial cell; ENS, enteric nervous system; FBS, fetal bovine serum; GDNF, glial cell line-derived neurotrophic factor; GFAP, glial fibrillary acidic protein; MAP2, microtubule-associated protein 2; nNOS, neuronal nitric oxide synthase; PFA, paraformaldehyde; α-SMA, α-smooth muscle actin; TBS, Tris-buffered saline; TGFβ, transforming growth factor β; Tuj1, βIII-tubulin.

© 2016 The Authors. The Journal of Physiology © 2016 The Physiological Society

DOI: 10.1113/JP271989

Introduction

The enteric nervous system (ENS) is composed of enteric neurons and enteric glial cells (EGCs), which are organised as interconnected ganglia localised along the gut and integrate local and systemic signals to control gastrointestinal functions, such as motility, secretion, intestinal permeability and epithelial cell proliferation (Schemann & Neunlist, 2004). Enteric neurons and EGCs are derived from precursors that originate in the neural crest, migrate to the gut, and undergo a long process of development and maturation (Burns & Pachnis, 2009; Gershon, 2010). In rodents, after the migration of neural precursor cells is completed during the embryonic period, major changes in enteric neuron morphology, electrophysiological properties, expression of neurotransmitters and neuroglial circuitry occur postnatally from birth to weaning (de Vries *et al.* 2010; Foong *et al.* 2012). Remarkably, these changes are correlated with functional maturation of gut motility, supporting the critical role of ENS postnatal development in digestive functions (de Vries *et al.* 2010). Although a great deal is known about the early events in enteric neuron development (Enomoto *et al.* 1998; Uesaka *et al.* 2007, 2013; Burns & Pachnis, 2009; Hao *et al.* 2010; Foong *et al.* 2015), much less is known about later-acting mechanisms, particularly those involved in the maturation and patterning of the neuronal network. Several neuronal intrinsic factors have been identified as key players for the elaboration of enteric neuron wiring, including the transcriptional cofactor homeodomain interacting protein kinase 2 (Chalazonitis *et al.* 2011), the planar cell polarity genes *Celsr3* and *Fzd3* (Sasselli *et al.* 2013), and the motor protein of the kinesin superfamily protein KIF26A (Zhou *et al.* 2009). Beside intrinsic factors, extrinsic factors from the neuronal microenvironment are also probably involved in shaping the neuronal circuitry. In this respect, EGCs are intimately associated with neurons within enteric ganglions and are therefore well positioned to regulate neuronal maturation (Gulbransen & Sharkey, 2012). EGCs are not only in close proximity to neurons but also envelop neuronal cell bodies and axon bundles, a configuration that is highly reminiscent of the close relationship between astrocytes and neurons in the CNS (Jessen & Mirsky, 1983). Recent studies have shown that astrocytes can use both secreted and contact-mediated signals to control several processes important for neural circuit maturation, including dendritic shaping, axon guidance and synapse formation (Murai *et al.* 2003; Procko & Shaham, 2010; Clarke & Barres, 2013; Molofsky *et al.* 2014). The fact that EGCs and astrocytes share morphological features and electrophysiological properties (Hanani *et al.* 2000) and express similar proteins, including the intermediate filament glial fibrillary acidic protein (GFAP) and the calcium-binding protein S100β (Jessen & Mirsky, 1980; Ferri *et al.* 1982), led to the concept that EGCs might share many features of CNS astrocytes (Gulbransen & Sharkey, 2012). Recent studies have shown important changes in EGC phenotype during the postnatal period (Kabouridis *et al.* 2015; Cossais *et al.* 2016), which also corresponds to a key developmental window for enteric neuron maturation. So far, whether EGCs, similarly to astrocytes in the CNS, are involved in the maturation of the developing enteric neuronal circuit is currently unknown. A major obstacle in directly addressing this question is the difficulty in obtaining a valuable cell model in which neurons can be isolated and maintained without EGCs. To address this issue, we first adapted a cell culture method previously developed for CNS neurons, in which neurons were grown on glass coverslips suspended above an astrocyte feeder layer (Kaech & Banker, 2006). Adapting this method to the ENS, we showed that EGCs exert an essential role in the formation of the axonal arborisation and of synaptic connections between enteric neurons. We further identified purinergic- and glial cell line-derived neurotrophic factor (GDNF)-dependent pathways in the effects mediated by EGCs.

Methods

Animals

Pregnant Sprague-Dawley rats were obtained on gestational day 15 (Janvier Labs, Le Genest-Saint-Isle, France). Rats were individually housed in cages on a 12:12-h light–dark cycle with free access to food and water. Mothers and their pups (10–14 pups/litters) were kept in the same conditions during the whole experiments. Day of birth was considered as postnatal day (P) 0. Pups were killed at P1, P7, P21 and P36. Pups were killed by decapitation (P1 and P7) or were anaesthetised with isoflurane (5 min; Abbot, Maidenhead, UK) and killed by cervical dislocation (P21 and P36). For cell culture, pregnant rats were anaesthetised using isoflurane and killed by cervical dislocation at gestational day 15, and the embryos were collected to proceed to cell culture. All protocols were carried out in accordance with French standard ethical guidelines for laboratory animals (Agreement no. 02476.01).

Cell culture and treatments

Mixed culture of the ENS. Primary culture of rat ENS was performed as previously described (Chevalier *et al.* 2008). Embryonic day 15 (E15) rat intestine were removed and finely diced in Hank's buffered salt solution and triturated mechanically using a scalpel. Tissue fragments were collected in Dulbecco's modified Eagle medium (DMEM)/F12 (1:1) medium (Life Technologies, Carlsbad, CA, USA) containing 50 μg ml^{-1} streptomycin and

© 2016 The Authors. The Journal of Physiology © 2016 The Physiological Society

50 U ml^{-1} penicillin and incubated for 15 min at 37°C in the same medium containing 0.25% trypsin (Invitrogen). After addition of 10% fetal bovine serum (FBS) to inactivate trypsin, the samples were incubated for 10 min at 37°C with 0.1% DNase I (Sigma, St Louis, MO, USA). After trituration and centrifugation for 10 min at 50 *g*, cells were plated in DMEM/F12 containing antibiotics and 10% FBS at a density of 2.4×10^5 cells cm^{-2} on 24-well plates previously coated with 0.5% gelatin (Sigma). After 24 h, the medium was replaced with the same medium without FBS but containing 1% of N-2 supplement (Invitrogen). Half of the medium was replaced every 2 days, and primary cultures were maintained for 12 days.

Neuro-glial coculture model and pharmacological treatment. First, a glial feeder layer was made up with EGCs or astrocytes. The EGCs were prepared from ENS cultures derived from the intestine of E15 rat embryos (Van Landeghem *et al.* 2011). Briefly, the primary cultures were trypsinised after 13 days of culture and seeded in serum-containing media after differential centrifugation. Following 7 days of culture, isolated areas of morphological glial-like cells were trypsinised using a cloning cylinder and seeded in culture flask in serum-containing media. After 1 month, the cultures were found to be immunoreactive for GFAP, Sox10 and S-100β (glia), but not for Tuj1, PGP9.5 (neurons) or α-SMA (myofibroblasts). This procedure yielded a purity of the EGC culture of ∼95 % according to the ratio of the number of Sox10-positive cells per number of DAPI-positive cells.

The astrocytes were prepared as described previously (Louveau *et al.* 2015). Briefly, the cortex were dissected from P1 newborn rat forebrains and dissociated with trypsin and DNase I. After filtration through a 70 μm nylon mesh, the resulting cell suspension was plated at a density of 35×10^3 cells cm^{-2} in DMEM containing 10% FBS, 100 UI ml^{-1} penicillin and 100 μg ml^{-1} streptomycin. Cells were maintained for 10–12 days. To constitute the glia feeder layer, EGCs and astrocytes were plated at a density of 7500 cells cm^{-2} in a 24-well plate, and maintained for 4 days in DMEM containing 10% FBS, 2 mM glutamine, 50 μg ml^{-1} streptomycin and 50 UI ml^{-1} penicillin. The medium was replaced with serum-free Neurobasal/B27 medium (Gibco, Waltham, MA, USA) 3 h before neuron culture. Rat enteric neuron culture was prepared from the intestine of E15 rat embryos as described above, and the dissociated cells were plated at 175,000 cells cm^{-2} on glass coverslips coated with poly-L-lysine (1 mg ml^{-1}, Sigma) in DMEM high glucose containing 10% FBS, 2 mM glutamine, 50 μg ml^{-1} streptomycin and 50 UI ml^{-1} penicillin. The coverslips were then transferred 3 h later to the wells containing the glial feeder layer and 3 μM 1-β-D-arabinofuranosylcytosine (AraC, 5 μM, Calbiochem, Billerica, MA, USA) were added 24 h later to prevent overgrowth of EGCs and myofibroblasts. The cells were maintained for up to 12 days.

To identify the pathway involved in EGC–neuron cross-talk, the selective purinergic $P2Y_1$ receptor antagonist MRS 2500 (1 μM; Tocris Bioscience, Bristol, UK) (Hechler *et al.* 2006), the transforming growth factor β (TGFβ) neutralizing antibody 2G7 which neutralises TGF-β1, -β2 and -β3 (10 μg ml^{-1}) (Arteaga *et al.* 1993), or the selective GDNF neutralizing antibody which neutralises human and rat GDNF (10 μg ml^{-1}; AB-212-NA, R&D Systems, Minneapolis, MN, USA) were added at 4 and 6 days *in vitro* (DIV). For control conditions, PBS or control IgG (10 μg ml^{-1}) were added in control wells. The cells were fixed at 7 DIV for Tuj1 immunostaining.

Immunostaining

Tissue. Segments of rat proximal colon were fixed in 0.1 M PBS containing 4% paraformaldehyde at room temperature for 3 h at 4°C. Whole mounts of longitudinal muscle and myenteric plexus were obtained by microdissection and were first permeabilised with PBS containing 4% horse serum and 0.5% Triton X-100. Tissues were then incubated with the following primary antibodies: rabbit anti-GFAP (2 μg ml^{-1}, Dako, Glostrup, Denmark) and mouse anti-Synapsin I (2 μg ml^{-1}, Synaptic Systems, Göttingen, Germany) for 12 h at room temperature. After several washes in PBS, tissues were incubated for 1 h at room temperature with the appropriate FITC-conjugated or Alexa 568-conjugated secondary antibodies diluted in PBS containing 1% horse serum. Tissues were washed with PBS and mounted with ProLong Gold Antifade Reagents with DAPI (Molecular Probes, Carlsbad, CA, USA).

Cell culture. Cells were fixed in PBS containing 4% paraformaldehyde for 15 min. Cells were permeabilised for 5 min at room temperature in 0.25% Triton-X-100 in PBS, washed twice with PBS, and incubated for 30 min at 37°C in PBS containing 10% BSA. Neurons were incubated overnight at 4°C with primary antibodies diluted in PBS containing 3% BSA and 0.02% azide. Antibodies used were as follows: mouse anti-Synapsin I (2 μg ml^{-1}, Synaptic Systems), rabbit anti-microtubule-associated protein 2 (MAP2; 1:1000, Millipore), mouse anti-βIII-tubulin (Tuj1, 1 μg ml^{-1}, Sigma), goat anti-choline acetyltransferase (ChAT; 1:200; Millipore), rabbit anti-neuronal nitric oxide synthase (nNOS; 1:1,000; Alexis Biochemicals, San Diego, CA, USA), mouse anti-HuC/D (1:500; Molecular Probes), rabbit anti-HuD (0.4 μg ml^{-1}; Santa Cruz Biotechnology, Santa Cruz, CA, USA), mouse anti-α-smooth muscle actin (α-SMA, 1 μg ml^{-1}, Abcam Inc., Cambridge, MA, USA), mouse anti-S100β (1:1000, Abcam), anti-active caspase 3 (1:2000, Sigma-Aldrich),

© 2016 The Authors. The Journal of Physiology © 2016 The Physiological Society

anti-PSD95 (10 μg ml^{-1}; Thermo Fisher Scientific). After washing, cells were incubated for 90 min at room temperature with the appropriate FITC-conjugated or Alexa 568-conjugated secondary antibodies diluted in PBS containing 3% BSA and 0.02% azide. Cells were washed with PBS and mounted with ProLong Gold Antifade Reagent with DAPI (Molecular Probes).

Western blot

Cells from cultures on coverslips or from mixed cultures were scrapped into cold PBS containing protease cocktail inhibitor, pelleted and resuspended in Laemmli buffer. Cell lysates were separated using the Invitrogen NuPage Novex Bis Tris MiniGels (4–12% bis Tris) with the Mes-SDS running buffer before electrophoretic transfer to nitrocellulose membranes with the iBlot2 Dry Blotting System (Life Technologies). Membranes were blocked for 1 h at 25°C in Tris-buffered saline-Tween 0.1% (TBST) (150 mM NaCl, 15 mM Tris, 4.6 mM Tris base, Tween 0.1%, pH 7.4) containing 5% non-fat dry milk and incubated overnight at 4°C with the primary antibodies: rabbit anti-PGP9.5 (Cedarlane, Burlington, Ontario, Canada; diluted 1:5000), rabbit anti-GFAP (Dako, diluted 1:5000). Bound antibodies were detected with a horseradish peroxidase-conjugated anti-rabbit antibody (Thermo Fisher Scientific; diluted 1: 5000) and visualised by chemiluminescence (Clarity Western ECL Substrate, Bio-Rad, Hercules, CA, USA) using a Gel-Doc imager and the Image Lab Software (Bio-Rad).

Ca^{2+} imaging

Neurons at 8 DIV were incubated at 37°C for 1 h with 1 μM Fluo-4/AM (Life Technologies) in Neurobasal/B27 medium supplemented with 2 mM glutamine, 50 μg ml^{-1} streptomycin and 50 UI ml^{-1} penicillin and 0.02% pluronic acid. The culture plate was then mounted on an inverted epifluorescence microscope (Olympus IX50) equipped with a digital camera (Olympus DP 71). After two washes with Neurobasal medium, the cells were stimulated with different compounds as follows: KCl (75 mM, Sigma), 2′(3′)-*O*-(4-benzoylbenzoyl)-ATP (BzATP, 100 μM, Sigma), dimethylphenylpiperazinium (DMPP, 10 μM, Sigma) and veratridin (30 μM, Sigma). For experiments involving TTX, the cells were pre-incubated for 30 min with 0.5 μM TTX (Sigma) before the stimulation. Fluo-4 was excited at 488 nm and its fluorescence emission was collected at 510 nm. Images were captured every 0.45 s for 3 min using Cell B imaging software (Olympus). Further analysis was achieved using Virtual dub and Image J software. Regions of interest (ROIs) were drawn over each neuron. Fluorescence intensity was measured and normalised to the basal fluorescence at the onset of the recording for each ROI.

Image analysis of immunostainings and quantification

To determine the number of neurons, myofibroblasts and EGCs, cell cultures were immunostained for HuC/D, α-SMA and S100β, respectively. Images were acquired with a ×20 objective using a digital camera (DP50, Olympus) coupled to a fluorescence microscope (BX51, Olympus). The camera was driven by Olympus DP-Soft version 3.2. Each cell type was scored and normalised to the total number of nuclei labelled with DAPI. For each experiment ($n = 6$), a total of 300 cells were counted. The number of neurons per field (Hu-positive cells) was counted on eight fields of view from a ×20 objective for each experiment ($n = 3$–6). To determine the number of ganglia, defined by at least two aggregated neurons, half of the surface coverslip was scanned with a ×10 objective and the number of ganglia was scored. The number of neurons per ganglion were scored on 10 ganglia per experiment ($n = 3$–6).

For Sholl analyses, pictures of Tuj1-labelled cells were acquired with a ×10 objective and a template of concentric circles 60, 100 and 200 μm from the ganglion centre was overlaid on the ganglion using Image J software. The number of axons crossing each circle was counted. For each experiment ($n = 3$–6), eight ganglia were analysed. To determine synapse density and size, images were acquired with a ×100 oil immersion objective. The same exposure time was used for all conditions, thereby ensuring accurate comparisons. The number of synapsin clusters per unit length of axon was determined with ImageJ software for 10 randomly selected axons per experiment ($n = 3$–6). The fluorescence intensity threshold for clusters was defined as at least two times the average intensity of fluorescence in the underlying neuronal process as previously described (Louveau *et al.* 2013).

GDNF detection

GDNF levels in cell lysate and conditioned medium from cultured EGCs were assessed by the ELISA kit '*GDNF E_{max}*' (Promega, Madison, WI, USA) designed for specific detection of GDNF, as less than 3% of cross-reactivity was detected with other neurotrophic factors. The conditioned medium from EGC cultures was concentrated five times with Amicon Centrifugal filter devices (Millipore) before ELISA analysis. To prepare EGC cell lysates, the cells were scraped, collected and lysed by sonication (2×5 s) in Tris-HCl 10 mM, pH 7.4. The suspension was centrifuged at 10,000 *g* for 30 min and the supernatant was collected for ELISA analysis.

Statistics

Data analysis and statistics were performed using Excel and GraphPad Prism 5. Values indicated are the mean ± SEM.

© 2016 The Authors. The Journal of Physiology © 2016 The Physiological Society

Group comparisons were made by the Mann–Whitney test, Kruskal–Wallis test with Dunn's *post hoc* test or by two-way ANOVA with Bonferroni *post hoc* test as indicated. The level of statistical significance was set at $^{*}P < 0.05$, $^{**}P < 0.01$ and $^{***}P < 0.001$.

Results

Parallel formation of the glial network with neuronal synaptic connectivity

Previous studies have shown a progressive increase in expression of glial proteins, such as GFAP and S100β, between P1 and P21 in the rat colon, suggesting that developmental maturation of EGCs occurs during this critical developmental window (Cossais *et al.* 2016). To determine the spatiotemporal relationships between EGC maturation and the formation of neuronal connectivity, we performed double immunostaining of whole mount preparations of rat colon for synapses, using the pre-synaptic marker synapsin I, and for EGC maturation, using GFAP labelling. At P1, only a few weakly stained synapsin I puncta were observed within the neuronal structures, while no GFAP staining was detected (Fig. 1). At P7, a robust synapsin I labelling was observed, which strikingly paralleled that of GFAP (Fig. 1). Both synapsin I and GFAP immunoreactivities were restricted to the ganglionic area. At P21 and P36, the extent of synapsin I and GFAP labelling further increased (Fig. 1). These data indicate a parallel developmental profile of GFAP expression in EGCs and synapse formation during the postnatal period, potentially implicating EGC maturation in the regulation of neuronal connectivity in the ENS.

A novel enteric neuron–EGC coculture model to study neuron–glia interaction

The coordinated developmental profile of EGCs and synapses suggested that EGCs might play an important role in neuronal maturation and connectivity. To directly study the influence of EGCs on neuronal maturation, we designed a culture system highly enriched in enteric neurons which could grow in the presence or absence of EGCs. Specifically, dissociated cells prepared from E15 rat intestines were plated on a coverslip placed above a layer of EGCs, resulting in a non-contact culture model (Fig. 2*A*). The percentage of neurons, EGCs and myofibroblasts was determined on the coverslips at 1, 4, 8 and 12 DIV by immunofluorescence with antibodies to HuC/D, S100β and αSMA, respectively (Fig. 2*B*). First, S100β-positive cells were never detected in this cell culture system whatever the stage of culture. Similarly, no labelled cell was observed with GFAP antibody. At 1 DIV, the neurons accounted for 10.5 ± 1.2% of the total cells (determined by DAPI staining), while the majority of the cells were myofibroblasts (45.2 ± 8.0%). At this stage, neurons remained isolated from each other and no ganglion was formed (Fig. 2*B*, *C*). From 3 DIV, the myofibroblasts progressively died and detached from the coverslips. At 4 DIV, a similar percentage of neurons and myofibroblasts was found (Fig. 2*C*). At this stage, neurons are grouped within ganglia containing an average of 10.1 ± 0.7 neurons. At 8 DIV, neurons represented the main cell type (82.6 ± 5.6% of total cells), and this was maintained at 12 DIV (87.2 ± 3.5% of total cells; Fig. 2*B*, *C*). To further confirm the lack of EGCs in this culture model, cells grown on glass coverslips were

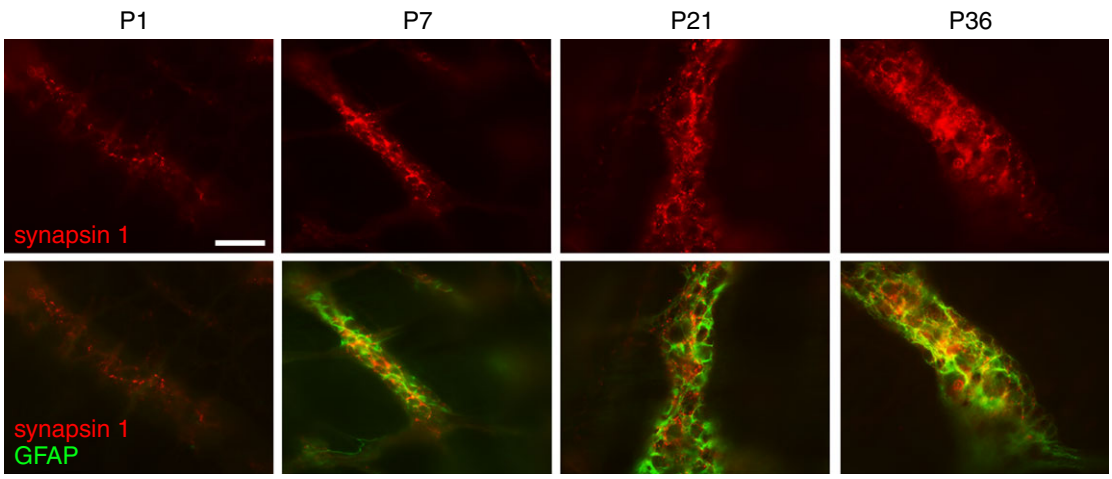

Figure 1. Parallel developmental profile of synapses and GFAP expression in EGCs during the postnatal period
Distribution of synapsin I (red) and GFAP (green) immunoreactivity in the myenteric plexus of rat colon from P1 to P36. Scale bar = 100 μm. [Colour figure can be viewed at wileyonlinelibrary.com]

© 2016 The Authors. The Journal of Physiology © 2016 The Physiological Society

collected at 8 DIV to analyse by Western blot the expression of neuronal (PGP9.5) and glial (GFAP) proteins (Fig. 2*D*), and results were compared to mixed cultures. For a comparable loading of neurons between the two types of culture, as shown by a similar signal of the neuronal protein PGP9.5, GFAP was detected only in the mixed culture samples, but not in the cell culture grown on glass coverslips (Fig. 2*D*). Neuronal cell death was assessed in the developing cell culture by quantification of active caspase 3-immunopositive neuron number at 1, 4, 8 and 12 DIV (Fig. 2*E*). We found that 4.8 ± 1.3% of neurons (identified with Hu staining) at 1 DIV were immunopositive for active caspase 3, reached 10.9 ± 3.2% at 4 DIV and stabilised at this level until 12 DIV (Fig. 2*E*).

Together, these results suggest that the experimental conditions established in the present study resulted in a highly enriched neuronal culture.

Structural and functional maturation of isolated cultured neurons

We then analysed whether enteric neurons cultured in the conditions described above follow a proper developmental profile by acquiring key features of mature neurons. Neurons are highly polarised cells, which developmentally acquire a distinct molecular composition in axons, dendrites and synapses. Immunostaining of 8 DIV neurons with markers of neurons (Tuj1) and dendrites (MAP2) showed that MAP2 staining was strictly confined to the somatodendritic domain while Tuj1 staining labelled both the dendritic and the axonal arbour (Fig. 3*A*). The presynaptic marker synapsin I was distributed in clusters over the axonal arborisation and in ganglia (Fig. 3*B*, *C*). PSD95, a well-recognised post-synaptic marker in CNS neurons, was restricted to ganglia, corresponding to the site of neuronal cell bodies, but

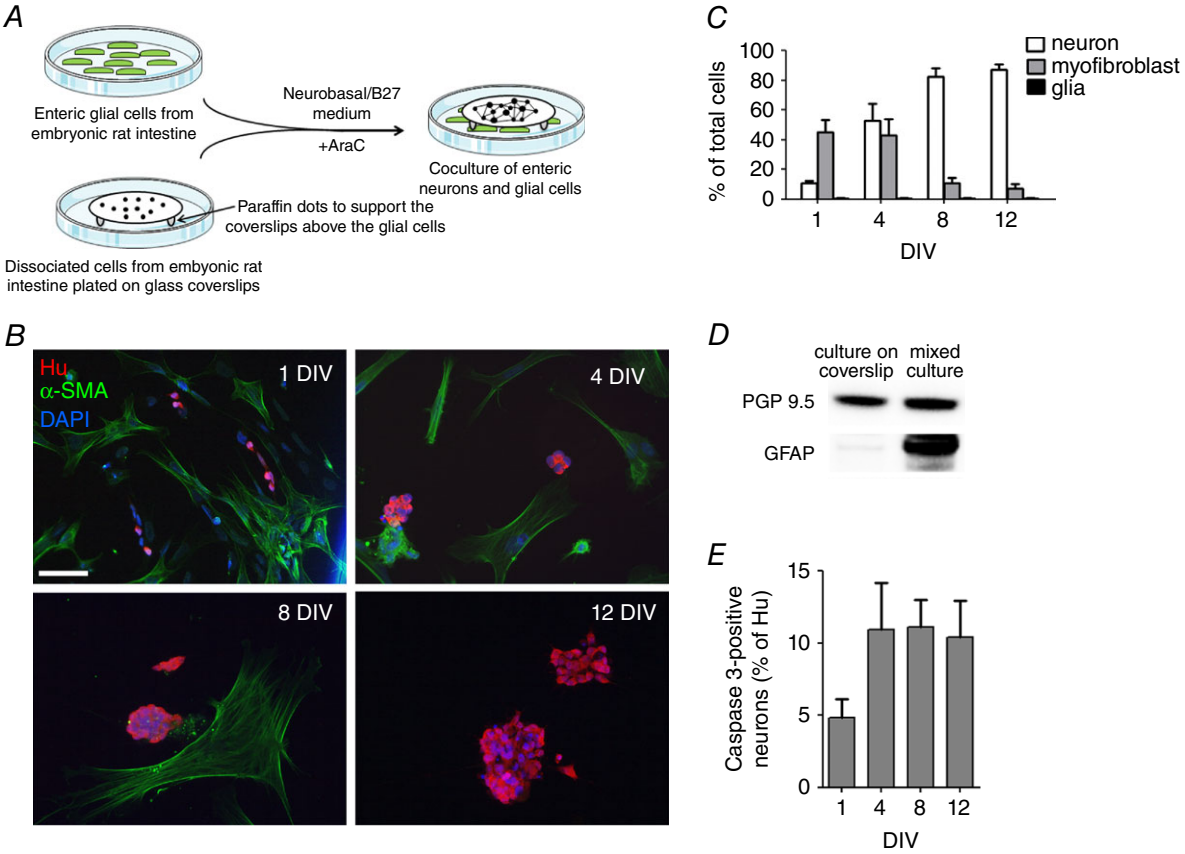

Figure 2. Neuron-enriched primary culture from E15 embryonic rat intestine
A, schematic summarizing the principle of the enteric neuron/glia coculture model. The two cell types are first prepared separately, and are then combined once the neurons have attached to the coverslips. The neurons and the glia remain separated by a narrow gap provided by the paraffin dots stuck on the glass coverslip. *B*, immunostaining for enteric neurons (Hu) and myofibroblasts (α-SMA) at 1, 4, 8 and 12 DIV in E15 embryonic rat intestine cultures grown on glass coverslips. Cell nuclei are labelled with DAPI. Scale bar = 50 μm. *C*, quantification of the percentage (mean ± SEM, $n = 6$) of enteric neurons, EGCs and myofibroblasts in cultures grown on glass coverslips. *D*, Western blot with PGP9.5 and GFAP antibodies of lysates from cultures grown on glass coverslips or from mixed cultures. *E*, neuronal cell death assessed by active caspase 3 immunostaining during *in vitro* development of the cell culture. Data are presented as mean ± SEM. [Colour figure can be viewed at wileyonlinelibrary.com]

© 2016 The Authors. The Journal of Physiology © 2016 The Physiological Society

absent in axonal processes, consistent with a postsynaptic localisation (Fig. 3*D*). Quantification of the colocalisation between synapsin I and PSD95 clusters in neuronal ganglia showed that 29.0 ± 3.8% of PSD95 clusters colocalised with synapsin I clusters, suggesting that a subset of synapses formed between enteric neurons comprises synapsin I-expressing elements and PSD95-expressing postsynaptic structures. Next, we examined the expression of markers for the key neuromediators/enzymes in the neuronal culture using antibodies against ChAT and nNOS to label cholinergic and nitrergic neurons, respectively. Both ChAT- and nNOS-positive neurons were observed (Fig. 3*E*). In particular, we showed that 11.7 ± 1.8 and 21.1 ± 1.6% of total neurons (identified with Hu staining) were immunopositive for nNOS at 8 and 12 DIV, respectively.

The capacity of the cultured neurons to respond to depolarisation and neuroligand stimulation was assessed by Ca^{2+} imaging with the fluorescent calcium indicator Fluo-4/AM on 8 DIV live neurons. Note that these experiments were carried out in the absence of the EGC feeder layer, thus allowing us to measure the direct

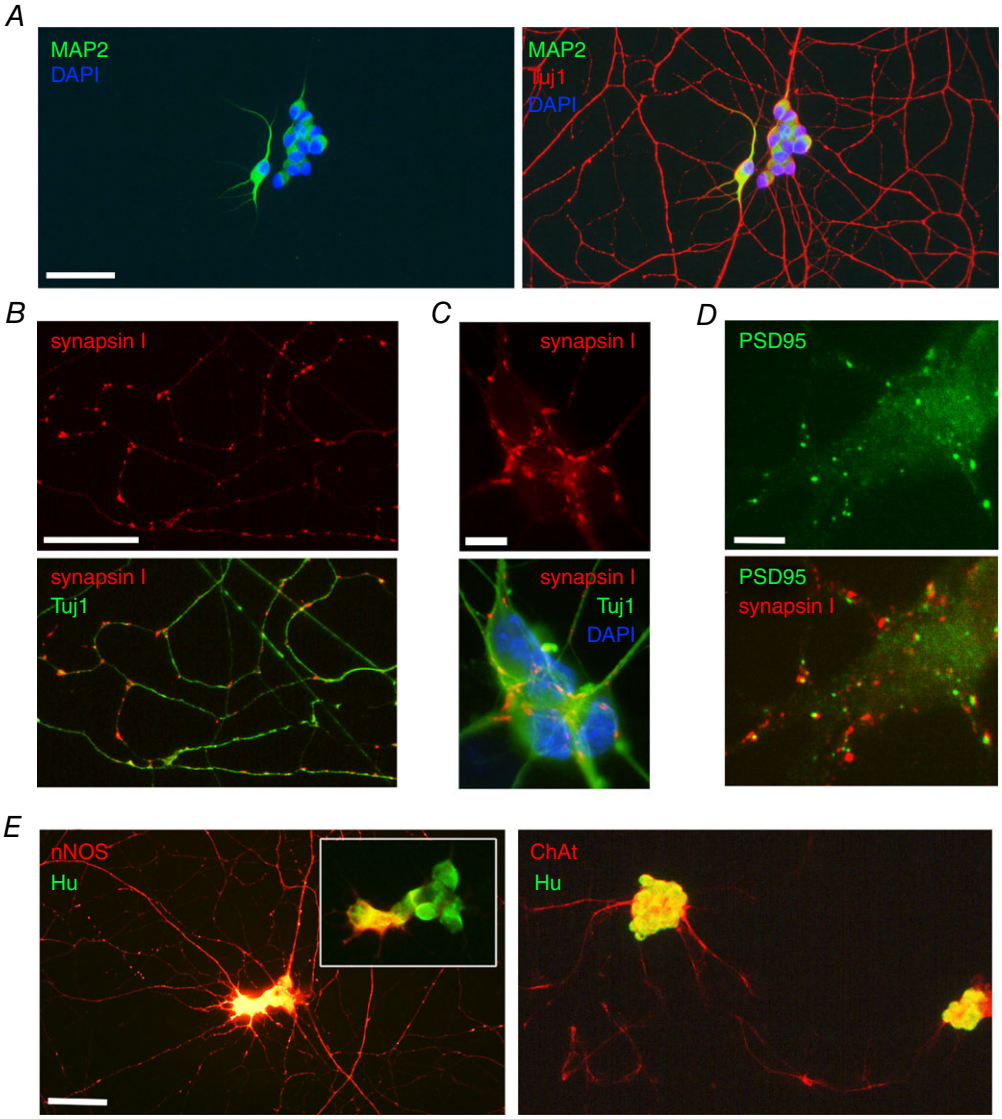

Figure 3. Primary cultures of E15 rat intestine grown on glass coverslips give rise to mature neurons
A, cultures were fixed at 8 DIV and immunostained with markers for neurons (Tuj1; red) and dendrites (MAP2; green). Cell nuclei are labelled with DAPI. *B* and *C*, immunostaining for Tuj1 (green) and the synaptic marker synapsin I (red) in a representative field of the axonal network (*B*) and in a ganglion (*C*). Cell nuclei are labelled with DAPI in *C*. *D*, immunostaining for the presynaptic marker synapsin I (red) and the postsynaptic marker PSD9.5 (green) in a ganglion. *E*, double immunostaining with the neuronal cell body marker HuC/D (green) and either nNOS (red, left panel) or ChAT (red, right panel) at 8 DIV. The inset shows the ganglion imaged with a lower exposure time to better visualise nNOS-immunoreactive neuronal cell body. Scale bars = A, B, E: 15 μm; C, D: 5 μm. [Colour figure can be viewed at wileyonlinelibrary.com]

© 2016 The Authors. The Journal of Physiology © 2016 The Physiological Society

neuronal effects of the stimulations. Isolated enteric neurons displayed a rapid and transient Ca^{2+} response to high K^+ depolarisation (Fig. 4*A*, *B*). Similarly, application of the nicotinic cholinergic receptor agonist DMPP (10 μM) and of the purinergic receptor agonist BzATP (100 μM) induced a rapid intracellular Ca^{2+} increase (Fig. 4*B*). These data suggest that isolated cultured neurons are sensitive to depolarisation and that they express functional cholinergic and purinergic receptors. We then analysed the contribution of voltage-gated sodium channels in the response to KCl and neuroligand stimulation. First, the functional expression of the sodium channel was confirmed using the sodium channel activator veratridine (30 μM), which induced a Ca^{2+} increase in all neurons (Fig. 4*B*). Next, the impact of the pharmacological blockade of sodium channels by TTX (0.5 μM) was analysed on the Ca^{2+} response induced by veratridine, KCl, DMPP and BzATP (Fig. 4*C*). TTX treatment inhibited the veratridine- and KCl-induced Ca^{2+} response by 80.7 ± 3.1 and 39.9 ± 12.6% respectively (Fig. 4*C*). By contrast, Ca^{2+} responses induced by DMPP or BzATP were unaffected (Fig. 4*C*). Together, the data indicated that the culture methodology employed in this study resulted in a cell culture highly enriched in neurons, and that these neurons developed properly to achieve structural and functional maturation.

EGCs are involved in formation of the axonal arbour

To study the influence of EGCs on the maturation of enteric neurons, we cultured enteric neurons in the presence or absence of EGCs. A culture condition in which enteric neurons were cocultured with CNS astrocytes was also included. We studied early-stage developmental processes, such as neuronal differentiation and ganglia formation, and late-stage processes related to neuronal maturation, such as axonal arbour elaboration. First, neurons were fixed at 1 and 4 DIV, and were immunostained with the neuronal markers Tuj1 and HuC/D to

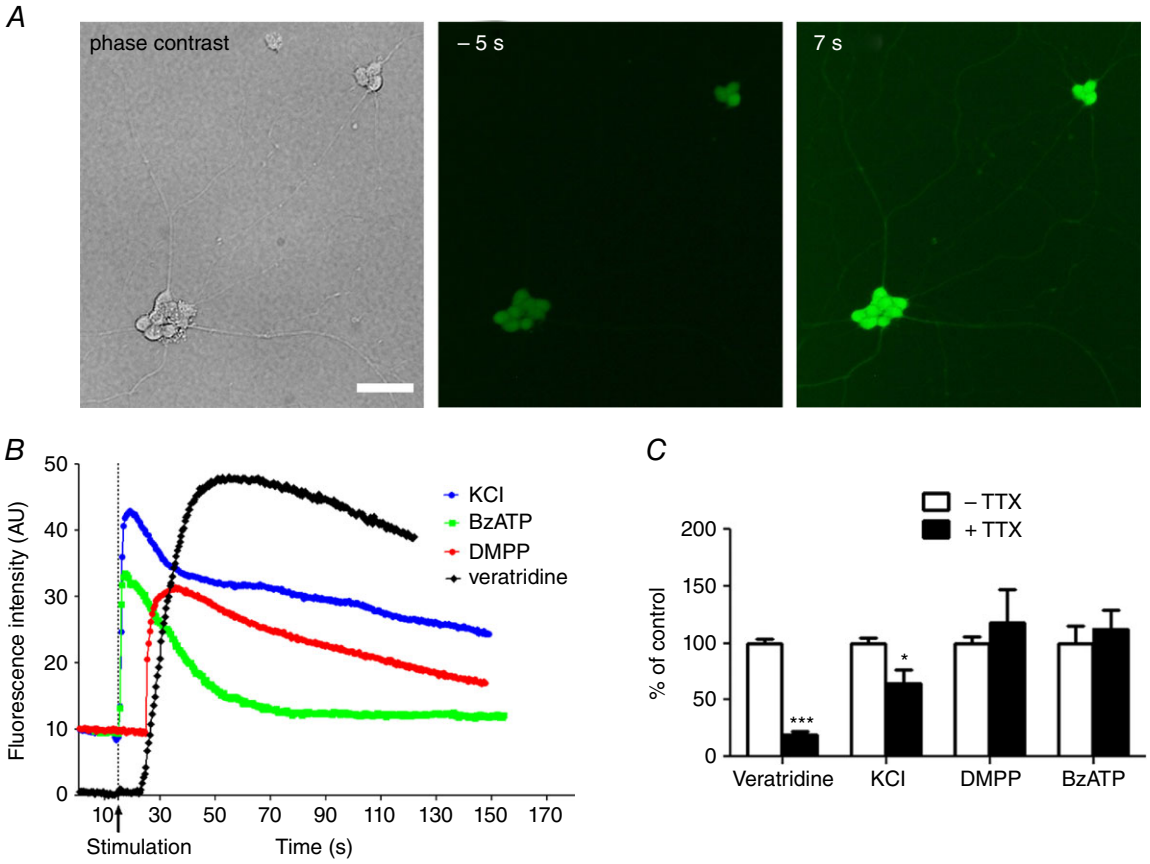

Figure 4. Ca^{2+} imaging of enteric neurons grown on glass coverslips
A, phase contrast and fluorescence images of a field containing two neuronal ganglia. Neurons were loaded with Fluo-4/AM and exposed to 75 mM KCl. Images were taken 5 s before (−5 s) and 7 s after (7 s) KCl application. Scale bar = 15 μm. *B*, representative traces of Ca^{2+} response evoked by 75 mM KCl, 10 μM DMPP, 100 μM BzATP or 30 μM veratridine. *C*, quantification of the amplitude of the Ca^{2+} response induced by veratridine, KCl, DMPP and BzATP in the absence and presence of TTX. Data are expressed as percentage of control condition without TTX (n = 12–25 cells from three independent experiments). $^*P < 0.05$, $^{***}P < 0.001$, Mann–Whitney. [Colour figure can be viewed at wileyonlinelibrary.com]

© 2016 The Authors. The Journal of Physiology © 2016 The Physiological Society

quantify the numbers of differentiated neurons, ganglia and neurons per ganglia. No significant difference was observed for these three parameters between neurons cultured in the absence or in the presence of EGCs or astrocytes (Fig. 5*A*, *B*). Next, neurons were fixed at 4 and 8 DIV and immunostained for Tuj1 and HuC/D to assess axonal complexity by Sholl analysis (Fig. 5*A*, *C*). This analysis indirectly measures both axonal length and axonal branching, giving rise to a measure of axonal complexity. At 4 DIV, quantitative analysis revealed that enteric neurons cultured in the absence of EGCs or in the presence of astrocytes showed a reduced axonal complexity in the distal arborisation, measured at 200 μm, compared to neurons cultured in the presence of EGCs (Fig. 5*D*; $P < 0.01$, $n = 10$–20, two-way ANOVA with Bonferroni *post hoc* test). At 8 DIV, enteric neurons cocultured with EGCs or astrocytes developed a profuse axonal arborisation with multiple branching, while neurons cultured in the absence of glial cells failed to form an elaborated and branched axonal network (Fig. 5*A*). Sholl analysis of neurons cultured without glia indicated a statistically significant reduction in axonal complexity at the proximal (50 μm), intermediate (100 μm) and distal (200 μm) arborisation compared to neurons cultured with EGCs (Fig. 5*D*; $P < 0.001$, two-way ANOVA with Bonferroni *post hoc* test). Neurons cocultured with astrocytes exhibited a lower axonal complexity only at the more distal part of the axonal arbour, measured at 200 μm from the ganglion centre, compared to neurons cocultured with EGCs. (Fig. 5*D*; $P < 0.01$, two-way ANOVA with Bonferroni *post hoc* test). These data suggest that, *in vitro*, EGCs are dispensable for neuronal differentiation and the formation of ganglia but are required for the establishment of a complex axonal network, during both initiation (4 DIV) and maturation (8 DIV) stages.

EGCs regulate synapse density

To further study the effects of EGCs on neuronal maturation, the number and size of synapses within the axonal network were analysed in neurons cultured in the absence or presence of glial cells. The neurons were fixed at 8 DIV and immunolabelled for Tuj1 and synapsin I to label the axonal arbour and synapses, respectively (Fig. 6*A*). Neurons grown without glia showed a decreased number of synapses compared to neurons grown with EGCs or astrocytes (Fig. 6*B*; the number of synapsin I clusters per 100 μm of axon was 12.0 ± 1.1, 8.4 ± 0.5 and 2.4 ± 0.5 with EGCs, astrocytes or without glia, respectively; $P < 0.001$ Kruskal–Wallis test with Dunn's *post hoc* test). Although neurons cultured with astrocytes showed a trend towards a decrease in the number of synapses, the values did not reach statistical significance when compared to neurons cultured with EGCs (Fig. 6*B*). A reduction in the size of the synaptic clusters was observed for neurons cultured in the absence of glia compared to neurons cultured with EGCs (Fig. 6*C*).

We next analysed whether neurons grown in the absence of EGCs still retained their ability to respond to depolarisation. Live Ca^{2+} imaging was performed on neurons grown with or without EGCs. We found that despite the dramatic reduction in axonal complexity and synapse number, neurons grown without EGCs still maintained their capacity to respond to high K^+-induced depolarisation (Fig. 6*D*).

EGCs promote axonal complexity through purinergic- and GDNF-dependent pathways

Next, we aimed to identify the EGC-derived factors important for the patterning of the axonal arborisation. In the CNS, TGFβ, GDNF and purinergic $P2Y_1$ receptor ($P2Y_1R$) signalling are important pathways in axonal outgrowth through mechanisms involving neuron–astrocyte crosstalk (Saavedra *et al.* 2006; Ng, 2008; del Puerto *et al.* 2012). We therefore examined in neuron–EGC cocultures whether blockade of each of these pathways between 4 and 6 DIV would affect the axonal arborisation. Quantification of the axonal complexity determined by Sholl analysis indicated that blockade of the TGFβ signalling by a TGFβ neutralizing antibody had no effect as compared to control neurons or neurons incubated with a control IgG (Fig. 7*A*, *B*). By contrast, blockade of GDNF by a neutralizing antibody reduced the axonal complexity in the distal part (200 μm) of the axonal arbour compared to control neurons or neurons treated with a control IgG (Fig. 7*A*, *B*; $^*P < 0.05$, two-way ANOVA with Bonferroni *post hoc* test). In addition, MRS 2500, a $P2Y_1R$ antagonist, induced a significant reduction of the axonal complexity in both the intermediate and the distal area of the axonal arborisation compared to control neurons (Fig. 7*A*, *B*; $^*P < 0.05$, $^\#P < 0.01$, two-way ANOVA with Bonferroni *post hoc* test). The number of neurons per ganglion was unaffected by the different treatments (Fig. 7*C*). Furthermore GDNF blockade by a neutralizing antibody between 4 and 6 DIV had no effect on the number of neurons per coverslip (control IgG: 948.5 ± 110; anti-GDNF antibody: 1080 ± 366, $P > 0.05$ Mann–Whitney). We next analysed GDNF production by EGCs using ELISA. GDNF was detected in cell lysate and conditioned culture medium from EGC culture composed of 95% EGCs (cell lysate: 234.8 ± 39.6 pg ml^{-1}; conditioned medium: 62.5 ± 5.0 pg ml^{-1}; Fig. 7*D*), indicating that EGCs produce and release GDNF.

Discussion

Our findings establish a highly enriched enteric neuronal culture from dissociated embryonic rat intestine. The neurons were cultured in indirect coculture with EGCs,

© 2016 The Authors. The Journal of Physiology © 2016 The Physiological Society

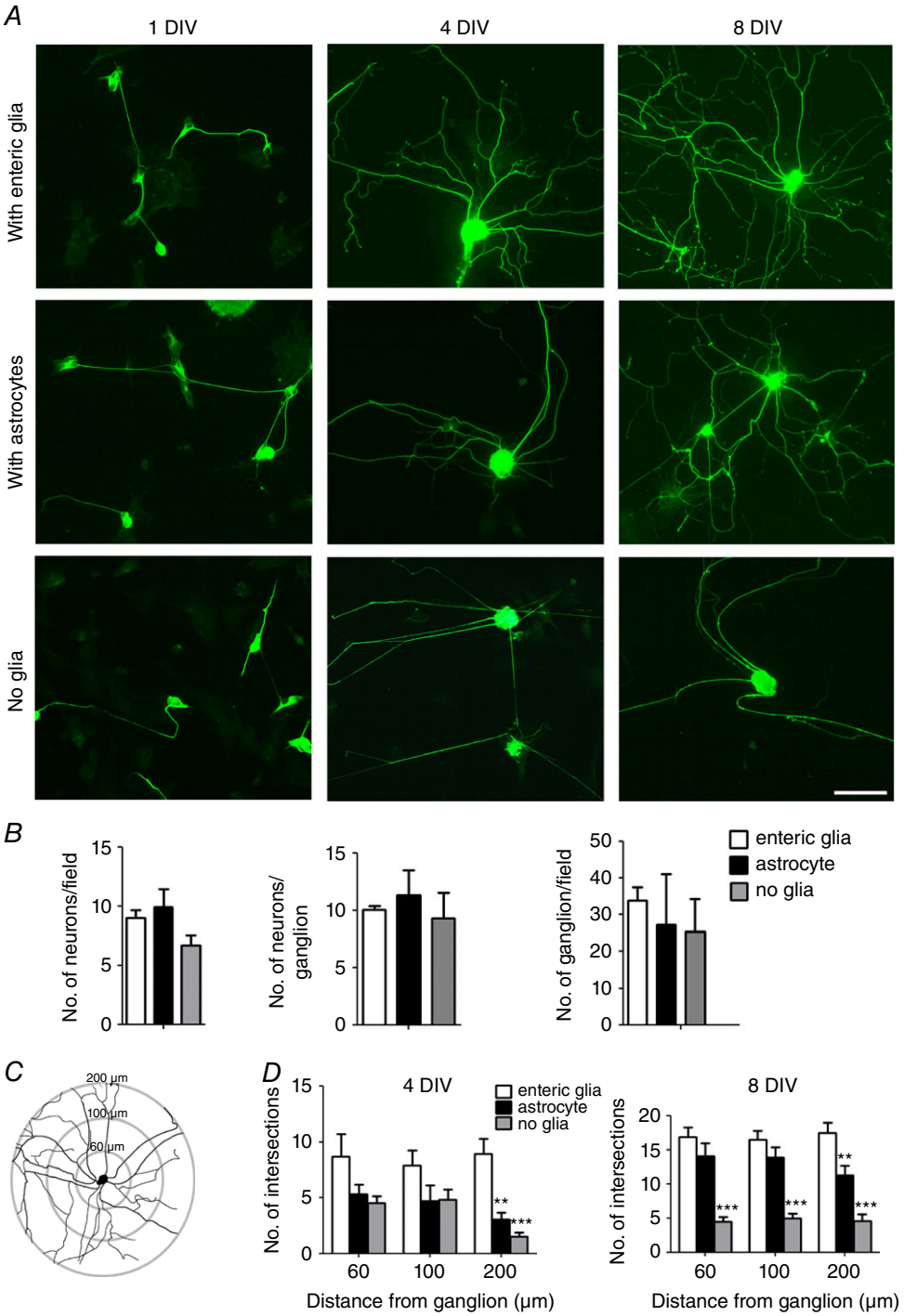

Figure 5. EGCs are required for the formation of a complex axonal arbour
A, enteric neurons grown on glass coverslips were cultured in the presence of EGCs, astrocytes or without glia. Cells were fixed at 1, 4 and 8 DIV and immunolabelled with Tuj1 antibody. Scale bar = 40 μm. *B*, enteric neurons cocultured with EGCs, astrocytes or without glia were immunolabelled with HuC/D at 1 DIV to quantify the number of neurons per field and at 4 DIV to quantify the number of neurons per ganglion and the number of ganglions per field. Data are mean ± SEM ($n = 6$), $P > 0.05$, Kruskal–Wallis with Dunn's *post hoc* test. *C*, Sholl axon analysis was used to measure axon complexity. Concentric circles were placed at 60, 100 and 200 μm from the ganglion centre, and the number of axonal intersections within each circle was counted. *D*, quantification of the number of intersections with each circle for enteric neurons cocultured with EGCs, astrocytes or without glial cells. The data are presented as mean ± SEM ($n = 15$ ganglia from three independent experiments). $^{**}P < 0.01$, $^{***}P < 0.001$ compared with neurons cocultured with EGCs, two-way ANOVA with Bonferroni *post hoc* test. [Colour figure can be viewed at wileyonlinelibrary.com]

© 2016 The Authors. The Journal of Physiology © 2016 The Physiological Society

allowing for the exchange of molecules between both cell types. This model enabled us to demonstrate the critical role of EGCs in the formation of the axonal arborisation and of synaptic connections between enteric neurons. We found that the effects played by EGCs on neuronal maturation were mediated in part through purinergic $P2Y_1R$- and GDNF-dependent pathways. This study describes a novel and valuable ENS culture model to study neuron–glia interactions during development and identifies EGC-derived factors important for neuronal maturation.

Here, we first present a novel enteric neuron–glia coculture method resulting in a highly enriched neuronal population, allowing us therefore to uniquely study the impact of EGCs on neuronal development. The combined use of a defined culture medium favouring neuronal survival and of the anti-mitotic compound AraC led to elimination of the EGCs and of the majority of intestinal smooth muscle cells by 8 DIV. Enteric neurons grown in such conditions showed several structural and phenotypic hallmarks of proper development and maturation, including dendrite/axon polarisation, the presence of synapses and the neurotransmitter specification as assessed by the expression of ChAT and nNOS. In addition, Ca^{2+} elevation in response to depolarisation, activation of voltage-gated sodium channels or to cholinergic and purinergic activation provided evidence that enteric neurons grown in the absence of direct contact with EGCs retain their typical neuronal functions. The approaches widely used so far for ENS *in vitro* studies have employed explant cultures of enteric ganglia (Jessen *et al.* 1983), organotypic cultures (Natarajan *et al.* 1999) and mixed cultures of dissociated gut (Chevalier *et al.* 2008). Although all these culture models have proven valuable tools for studying ENS development and functions, they all contain a heterogeneous cell population, including intestinal smooth muscle cells, enteric neurons and EGCs, which hamper the study of the cell-to-cell interactions between the different cell types. Other ENS culture methodologies have been previously developed to limit cell diversity. Immunoselection of $p75^{NTR}$-positive cells from embryonic gut tissue resulted in the isolation of neural precursor cells, giving rise to a cell culture enriched in enteric

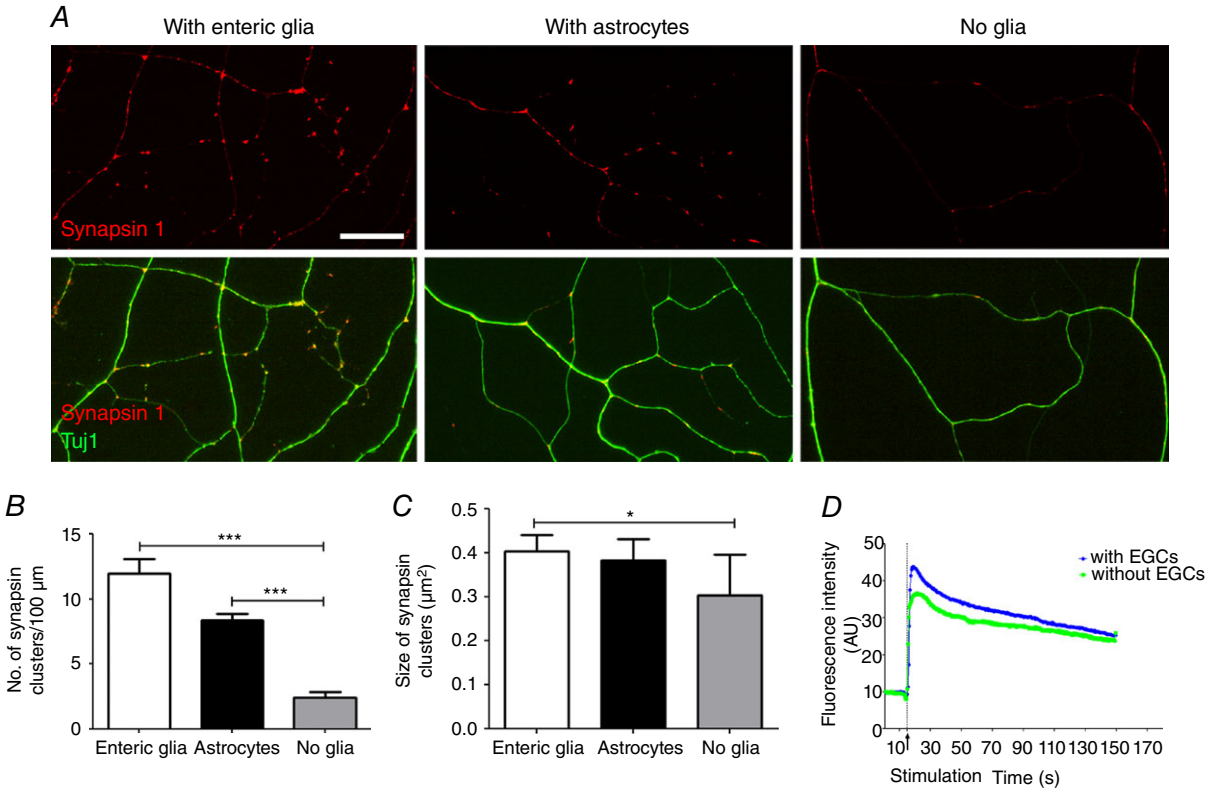

Figure 6. EGCs control the density of synaptic sites
A, enteric neurons grown on glass coverslips were cultured in the presence of EGCs, astrocytes or without glia and were fixed at 8 DIV for double immunolabelling with synapsin I and Tuj1 antibodies. Scale bar = 20 μm. *B* and *C*, quantification of the number of synapsin I clusters per 100 μm of axon (*B*) and size of synapsin I clusters (*C*). Data are mean ± SEM ($n = 4$ independent experiments). $^{*}P < 0.05$, $^{***}P < 0.001$, Kruskal–Wallis with Dunn's *post hoc* test. *D*, representative traces of Ca^{2+} response evoked by 75 mM KCl in neurons grown with or without EGCs. [Colour figure can be viewed at wileyonlinelibrary.com]

© 2016 The Authors. The Journal of Physiology © 2016 The Physiological Society

neurons and EGCs the first few days in culture, but in which smooth muscle cells appeared after 6 days of culture (Wu *et al.* 1999; Sato & Heuckeroth, 2008; Gisser *et al.* 2013). A procedure of myenteric explant culture of ganglia in which EGCs were eliminated through a combination of antibody complement-mediated cytolysis and anti-mitotic agent resulted after 20 DIV in a neuron-enriched culture (Bannerman *et al.* 1988). However, the relatively long procedure required to remove the EGCs prevented studies on early developmental processes. The new method described in the present study offers important advantages over the other approaches. First, enteric neuronal and glial cell populations were able to grow separately, therefore allowing us to study cell-to-cell interactions. Second, no cytotoxic procedure was required. Third, neuronal development can be studied from early to late stages of maturation.

A first finding is that the number of neurons per ganglion and the number of ganglia was similar in the presence or absence of EGCs, suggesting that EGCs might have limited impact on neuronal differentiation and ganglia formation in this coculture system, although some effects on selective neuronal subtypes could have gone undetected. This result is consistent with *in vivo* data showing that differentiation of enteric neurons occurs earlier than that of EGCs, and is therefore mostly independent of EGC-derived signals but rather requires molecules produced by gut mesenchyme (Young *et al.* 2003; Sasselli *et al.* 2012). By contrast, the absence of EGCs markedly diminished the complexity of the axonal arbour and the density of synapses. These findings indicate that EGCs, in part via secreted mediators, support late stages of neuronal development involved in the neuronal network expansion and connectivity. Accordingly,

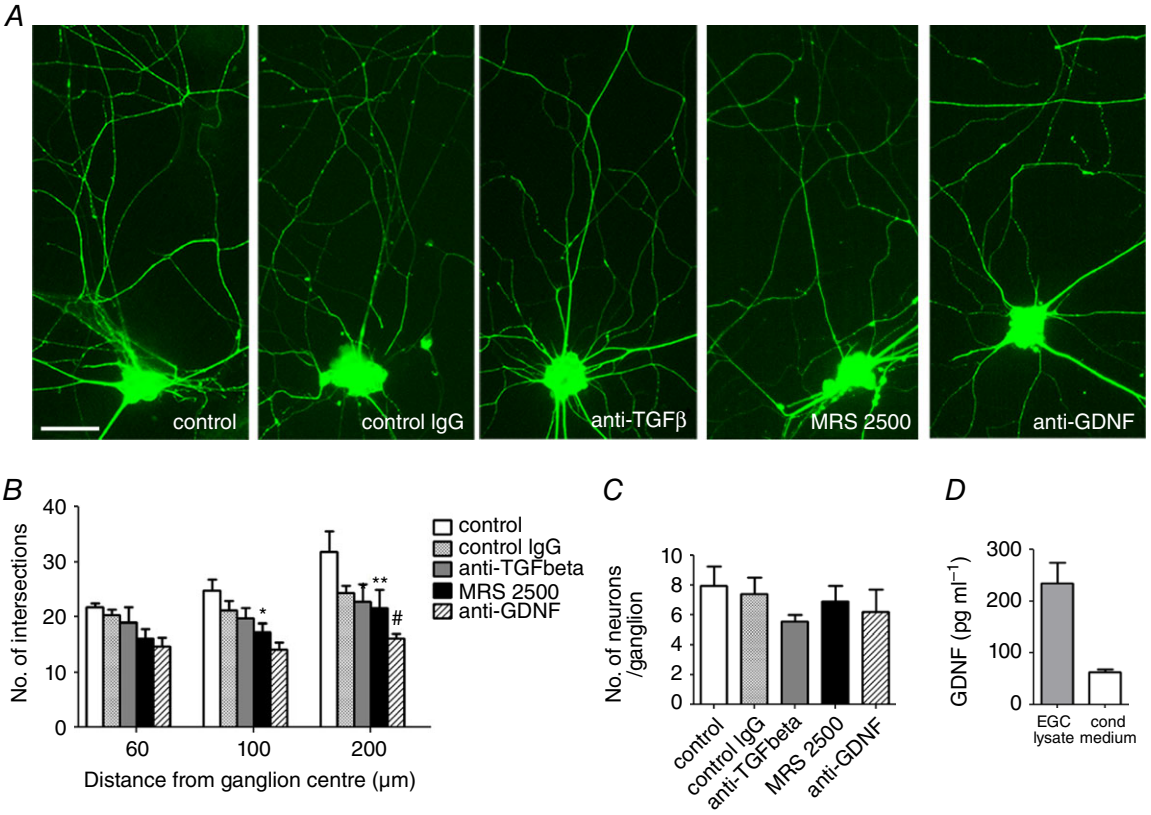

Figure 7. EGCs support axonal arbour complexity through purinergic $P2Y_1R$- and GDNF-dependent pathways

A, at 4 DIV, neurons cocultured with EGCs were treated for 4 days with control IgG (10 μg ml^{-1}), a TGFβ neutralizing antibody (10 μg ml^{-1}), the $P2Y_1R$ antagonist MRS 2500 (1 μM) or a GDNF neutralizing antibody (10 μg ml^{-1}). Neurons were fixed at 7 DIV and immunostained with Tuj1. Scale bar = 15 μm. *B*, quantification of the axonal complexity by Sholl analysis. The data represent the mean ± SEM (n = 15 ganglia from three independent experiments). $^{*}P < 0.05$, $^{**}P < 0.01$ compared with control neurons, $^{\#}P < 0.05$ compared with neurons treated with control IgG, two-way ANOVA with Bonferroni *post hoc* test. *C*, the number of neurons per ganglion was determined at 7 DIV by counting the number of Hu-positive cells per ganglion. Data are mean ± SEM (n = 3), $P > 0.05$, Kruskal–Wallis with Dunn's *post hoc* test. *D*, quantification of GDNF content analysed by ELISA in cell lysate and conditioned medium collected from EGC cultures. Values are mean ± SEM (n = 3). [Colour figure can be viewed at wileyonlinelibrary.com]

© 2016 The Authors. The Journal of Physiology © 2016 The Physiological Society

we found that GFAP and synapsin I expression in the colon showed a similar progressive increase during the postnatal period, suggesting that glial and neuronal maturation exert a functional interplay during postnatal development. The increased GFAP expression during the postnatal period was shown to be concomitant with increased expression of S100β (Cossais *et al.* 2016), suggesting that this parallel time-dependent regulation of glial protein expression reflects EGC postnatal maturation. In adults, phenotypic heterogeneity of the EGCs has been demonstrated by showing the existence of subsets of EGCs with differential expression of glial proteins such as S100β, GFAP and proteolipid protein 1 (Boesmans *et al.* 2015; Rao *et al.* 2015). Whether a subset of EGCs is selectively involved in the regulation of neuronal connectivity remains to be determined. Previous studies have reported the importance of EGCs in the biology and function of enteric neurons. Neurochemical coding (Aube *et al.* 2006), release and degradation of neuroactive substances (Sarosi *et al.* 1998; Nagahama *et al.* 2001; Fletcher *et al.* 2002), and neuroprotection (Abdo *et al.* 2010, 2012) have all been shown to be modulated by EGCs. In this study, we demonstrated a novel function of EGCs in shaping neuronal circuitry, thereby extending the importance of glia–neuron communication in ENS functions.

The low level of synapses detected in colonic myenteric neurons of the newborn rat is consistent with the absence of a contractile response induced by electrical field stimulation in rat colon at P1 (de Vries *et al.* 2010). The first significant response was observed between P7 and P14 (de Vries *et al.* 2010), in correlation with the emergence of synapses as observed in the present study. In newborn mice, the spontaneous colonic motility characterised by small erratic contractions has been found to be independent of neuronal activity but mediated by smooth muscle cell intrinsic activity (Roberts *et al.* 2007). The first mature patterns of colonic motility, which are controlled by neuronal activity, are detected at P10 (Roberts *et al.* 2007). Whether the establishment of the neurally dependent colonic motility in mice also correlates with synapse formation remains to be determined.

Another important finding of our study was that blockade of the GDNF and purinergic $P2Y_1R$ pathways decreased the axonal complexity of enteric neurons, without changing the number of neuronal cell bodies. Previous studies have shown that the addition of GDNF to mixed cultures of ENS or the transgenic expression of GDNF in EGCs in mice induced an increase in neuron and axon numbers (Wang *et al.* 2010; Rodrigues *et al.* 2011). The increased neuron number reported in these studies probably reflected the neurogenic and prosurvival activity exerted by GDNF on neural precursor cells (Sanchez *et al.* 1996; Heuckeroth *et al.* 1998), which could consequently result in an increased axon number. Therefore, the possibility that GDNF could directly regulate axonal outgrowth remained an open question. In the present study, blockade of the GDNF pathway was performed between 4 and 7 DIV, a developmental period with prominent axonal outgrowth while neuronal differentiation is largely completed. Therefore, the decreased axonal complexity induced by GDNF blockade, without affecting neuron number, suggests that GDNF regulates the patterning of neuronal processes, independently of its activity on neuronal differentiation and survival. Our study demonstrated that EGCs are a source of GDNF as previously reported by others (von Boyen *et al.* 2006; Xiao *et al.* 2014). Besides EGCs, enteric smooth muscle cells and intestinal epithelial cells have also been shown to produce GDNF in the intestine (Rodrigues *et al.* 2011; Meir *et al.* 2015). The diversity of the cellular sources of GDNF expression, and consequently the different site of production of GDNF, together with the temporal regulation of its expression, have been proposed to underlie the multiple functions of GDNF throughout ENS development, ranging from neural crest cell migration, neuronal differentiation and neuronal process patterning (Wang *et al.* 2010; Sasselli *et al.* 2012). Considering the delayed differentiation of EGCs, as compared to enteric neurons, one hypothesis is that EGC-derived GDNF could be particularly dedicated to the maturation of the axonal network during the postnatal period.

The present study also showed the contribution of the $P2Y_1R$-mediated pathway in the maturation of enteric neurons. The implication of the purine-mediated signalling in neuronal maturation has been demonstrated in the CNS by showing that ATP released from astrocytes exerts a trophic effect on cortical neurons, through activation of the neuronal $P2Y_1R$ (Cotrina *et al.* 2000; del Puerto *et al.* 2012). In the ENS, it has been shown that EGCs can release ATP, triggering intercellular Ca^{2+} waves (Zhang *et al.* 2003), and that ATP and its purine metabolites act as neurotransmitter mediating fast synaptic transmission (Galligan & Bertrand, 1994). The inhibitory effect of the $P2Y_1R$ antagonist on axonal complexity shown in the present study suggests that activity-dependent mechanisms might be involved in the regulation of the axonal outgrowth and patterning.

Our results support the idea that EGC deficiency in gliotransmitter production or release would impact neuronal morphogenesis, and ultimately ENS functioning. Interestingly, disruption of EGCs in mice by a glial-specific deletion of connexin-43 hemichannels or by autoimmune-mediated destruction induced alterations of gastrointestinal motility (Aube *et al.* 2006; McClain *et al.* 2014). Conversely, patients with slow-transit constipation exhibited a decreased number of EGCs (Bassotti *et al.* 2007). In light of the present results and given that anomalies in neurite outgrowth and neuronal connectivity

© 2016 The Authors. The Journal of Physiology © 2016 The Physiological Society

have been linked to gastrointestinal disorders (Sasselli *et al.* 2013; Dothel *et al.* 2015), one can envisage that alteration of EGCs might in turn affect the maturation of enteric neurons, suggesting that gliopathy-mediated neuronal remodelling might be involved in gastrointestinal disorders.

References

Abdo H, Derkinderen P, Gomes P, Chevalier J, Aubert P, Masson D, Galmiche JP, Vanden Berghe P, Neunlist M & Lardeux B (2010). Enteric glial cells protect neurons from oxidative stress in part via reduced glutathione. *FASEB J* **24**, 1082–1094.

Abdo H, Mahe MM, Derkinderen P, Bach-Ngohou K, Neunlist M & Lardeux B (2012). The omega-6 fatty acid derivative 15-deoxy-δ(1)(2),(1)(4)-prostaglandin J2 is involved in neuroprotection by enteric glial cells against oxidative stress. *J Physiol* **590**, 2739–2750.

Arteaga CL, Hurd SD, Winnier AR, Johnson MD, Fendly BM & Forbes JT (1993). Anti-transforming growth factor (TGF)-β antibodies inhibit breast cancer cell tumorigenicity and increase mouse spleen natural killer cell activity. Implications for a possible role of tumor cell/host TGF-β interactions in human breast cancer progression. *J Clin Invest* **92**, 2569–2576.

Aube AC, Cabarrocas J, Bauer J, Philippe D, Aubert P, Doulay F, Liblau R, Galmiche JP & Neunlist M (2006). Changes in enteric neurone phenotype and intestinal functions in a transgenic mouse model of enteric glia disruption. *Gut* **55**, 630–637.

Bannerman PG, Mirsky R & Jessen KR (1988). Establishment and properties of separate cultures of enteric neurons and enteric glia. *Brain Res* **440**, 99–108.

Bassotti G, Villanacci V, Nascimbeni R, Asteria CR, Fisogni S, Nesi G, Legrenzi L, Mariano M, Tonelli F, Morelli A & Salerni B (2007). Colonic neuropathological aspects in patients with intractable constipation due to obstructed defecation. *Mod Pathol* **20**, 367–374.

Boesmans W, Lasrado R, Vanden Berghe P & Pachnis V (2015). Heterogeneity and phenotypic plasticity of glial cells in the mammalian enteric nervous system. *Glia* **63**, 229–241.

Burns AJ & Pachnis V (2009). Development of the enteric nervous system: bringing together cells, signals and genes. *Neurogastroenterol Motil* **21**, 100–102.

Chalazonitis A, Tang AA, Shang Y, Pham TD, Hsieh I, Setlik W, Gershon MD & Huang EJ (2011). Homeodomain interacting protein kinase 2 regulates postnatal development of enteric dopaminergic neurons and glia via BMP signaling. *J Neurosci* **31**, 13746–13757.

Chevalier J, Derkinderen P, Gomes P, Thinard R, Naveilhan P, Vanden Berghe P & Neunlist M (2008). Activity-dependent regulation of tyrosine hydroxylase expression in the enteric nervous system. *J Physiol* **586**, 1963–1975.

Clarke LE & Barres BA (2013). Emerging roles of astrocytes in neural circuit development. *Nat Rev Neurosci* **14**, 311–321.

Cossais F, Durand T, Chevalier J, Boudaud M, Kermarrec L, Aubert P, Neveu I, Naveilhan P & Neunlist M (2016). Postnatal development of the myenteric glial network and its modulation by butyrate. *Am J Physiol Gastrointest Liver Physiol* **310**, G941–951.

Cotrina ML, Lin JH, Lopez-Garcia JC, Naus CC & Nedergaard M (2000). ATP-mediated glia signaling. *J Neurosci* **20**, 2835–2844.

de Vries P, Soret R, Suply E, Heloury Y & Neunlist M (2010). Postnatal development of myenteric neurochemical phenotype and impact on neuromuscular transmission in the rat colon. *Am J Physiol Gastrointest Liver Physiol* **299**, G539–547.

del Puerto A, Diaz-Hernandez JI, Tapia M, Gomez-Villafuertes R, Benitez MJ, Zhang J, Miras-Portugal MT, Wandosell F, Diaz-Hernandez M & Garrido JJ (2012). Adenylate cyclase 5 coordinates the action of ADP, P2Y1, P2Y13 and ATP-gated P2X7 receptors on axonal elongation. *J Cell Sci* **125**, 176–188.

Dothel G, Barbaro MR, Boudin H, Vasina V, Cremon C, Gargano L, Bellacosa L, De Giorgio R, Le Berre-Scoul C, Aubert P, Neunlist M, De Ponti F, Stanghellini V & Barbara G (2015). Nerve fiber outgrowth is increased in the intestinal mucosa of patients with irritable bowel syndrome. *Gastroenterology* **148**, 1002–1011.e4.

Enomoto H, Araki T, Jackman A, Heuckeroth RO, Snider WD, Johnson EM, Jr & Milbrandt J (1998). GFRα1-deficient mice have deficits in the enteric nervous system and kidneys. *Neuron* **21**, 317–324.

Ferri GL, Probert L, Cocchia D, Michetti F, Marangos PJ & Polak JM (1982). Evidence for the presence of S-100 protein in the glial component of the human enteric nervous system. *Nature* **297**, 409–410.

Fletcher EL, Clark MJ & Furness JB (2002). Neuronal and glial localization of GABA transporter immunoreactivity in the myenteric plexus. *Cell Tissue Res* **308**, 339–346.

Foong JP, Hirst CS, Hao MM, McKeown SJ, Boesmans W, Young HM, Bornstein JC & Vanden Berghe P (2015). Changes in nicotinic neurotransmission during enteric nervous system development. *J Neurosci* **35**, 7106–7115.

Foong JP, Nguyen TV, Furness JB, Bornstein JC & Young HM (2012). Myenteric neurons of the mouse small intestine undergo significant electrophysiological and morphological changes during postnatal development. *J Physiol* **590**, 2375–2390.

Galligan JJ & Bertrand PP (1994). ATP mediates fast synaptic potentials in enteric neurons. *J Neurosci* **14**, 7563–7571.

Gershon MD (2010). Developmental determinants of the independence and complexity of the enteric nervous system. *Trends Neurosci* **33**, 446–456.

Gisser JM, Cohen AR, Yin H & Gariepy CE (2013). A novel bidirectional interaction between endothelin-3 and retinoic acid in rat enteric nervous system precursors. *PLoS One* **8**, e74311.

Gulbransen BD & Sharkey KA (2012). Novel functional roles for enteric glia in the gastrointestinal tract. *Nat Rev Gastroenterol Hepatol* **9**, 625–632.

Hanani M, Francke M, Hartig W, Grosche J, Reichenbach A & Pannicke T (2000). Patch-clamp study of neurons and glial

© 2016 The Authors. The Journal of Physiology © 2016 The Physiological Society

cells in isolated myenteric ganglia. *Am J Physiol Gastrointest Liver Physiol* **278**, G644–651.

Hao MM, Moore RE, Roberts RR, Nguyen T, Furness JB, Anderson RB & Young HM (2010). The role of neural activity in the migration and differentiation of enteric neuron precursors. *Neurogastroenterol Motil* **22**, e127–137.

Hechler B, Nonne C, Roh EJ, Cattaneo M, Cazenave JP, Lanza F, Jacobson KA & Gachet C (2006). MRS2500 [2-iodo-N6-methyl-(N)-methanocarba-2'-deoxyadenosine-3',5'-bisphosphate], a potent, selective, and stable antagonist of the platelet P2Y1 receptor with strong antithrombotic activity in mice. *J Pharmacol Exp Ther* **316**, 556–563.

Heuckeroth RO, Lampe PA, Johnson EM & Milbrandt J (1998). Neurturin and GDNF promote proliferation and survival of enteric neuron and glial progenitors *in vitro*. *Dev Biol* **200**, 116–129.

Jessen KR & Mirsky R (1980). Glial cells in the enteric nervous system contain glial fibrillary acidic protein. *Nature* **286**, 736–737.

Jessen KR & Mirsky R (1983). Astrocyte-like glia in the peripheral nervous system: an immunohistochemical study of enteric glia. *J Neurosci* **3**, 2206–2218.

Jessen KR, Saffrey MJ & Burnstock G (1983). The enteric nervous system in tissue culture. I. Cell types and their interactions in explants of the myenteric and submucous plexuses from guinea pig, rabbit and rat. *Brain Res* **262**, 17–35.

Kabouridis PS, Lasrado R, McCallum S, Chng SH, Snippert HJ, Clevers H, Pettersson S & Pachnis V (2015). Microbiota controls the homeostasis of glial cells in the gut lamina propria. *Neuron* **85**, 289–295.

Kaech S & Banker G (2006). Culturing hippocampal neurons. *Nat Protoc* **1**, 2406–2415.

Louveau A, Angibaud J, Haspot F, Opazo MC, Thinard R, Thepenier V, Baudouin SJ, Lescaudron L, Hulin P, Riedel CA & Boudin H (2013). Impaired spatial memory in mice lacking CD3ζ is associated with altered NMDA and AMPA receptors signaling independent of T-cell deficiency. *J Neurosci* **33**, 18672–18685.

Louveau A, Nerriere-Daguin V, Vanhove B, Naveilhan P, Neunlist M, Nicot A & Boudin H (2015). Targeting the CD80/CD86 costimulatory pathway with CTLA4-Ig directs microglia toward a repair phenotype and promotes axonal outgrowth. *Glia* **63**, 2298–2312.

McClain JL, Grubisic V, Fried D, Gomez-Suarez RA, Leinninger GM, Sevigny J, Parpura V & Gulbransen BD (2014). Ca^{2+} responses in enteric glia are mediated by connexin-43 hemichannels and modulate colonic transit in mice. *Gastroenterology* **146**, 497–507.e1.

Meir M, Flemming S, Burkard N, Bergauer L, Metzger M, Germer CT & Schlegel N (2015). Glial cell line-derived neurotrophic factor promotes barrier maturation and wound healing in intestinal epithelial cells in vitro. *Am J Physiol Gastrointest Liver Physiol* **309**, G613–624.

Molofsky AV, Kelley KW, Tsai HH, Redmond SA, Chang SM, Madireddy L, Chan JR, Baranzini SE, Ullian EM & Rowitch DH (2014). Astrocyte-encoded positional cues maintain sensorimotor circuit integrity. *Nature* **509**, 189–194.

Murai KK, Nguyen LN, Irie F, Yamaguchi Y & Pasquale EB (2003). Control of hippocampal dendritic spine morphology through ephrin-A3/EphA4 signaling. *Nat Neurosci* **6**, 153–160.

Nagahama M, Semba R, Tsuzuki M & Aoki E (2001). L-Arginine immunoreactive enteric glial cells in the enteric nervous system of rat ileum. *Biol Signals Recept* **10**, 336–340.

Natarajan D, Grigoriou M, Marcos-Gutierrez CV, Atkins C & Pachnis V (1999). Multipotential progenitors of the mammalian enteric nervous system capable of colonising aganglionic bowel in organ culture. *Development* **126**, 157–168.

Ng J (2008). TGF-β signals regulate axonal development through distinct Smad-independent mechanisms. *Development* **135**, 4025–4035.

Procko C & Shaham S (2010). Assisted morphogenesis: glial control of dendrite shapes. *Curr Opin Cell Biol* **22**, 560–565.

Rao M, Nelms BD, Dong L, Salinas-Rios V, Rutlin M, Gershon MD & Corfas G (2015). Enteric glia express proteolipid protein 1 and are a transcriptionally unique population of glia in the mammalian nervous system. *Glia* **63**, 2040–2057.

Roberts RR, Murphy JF, Young HM & Bornstein JC (2007). Development of colonic motility in the neonatal mouse-studies using spatiotemporal maps. *Am J Physiol Gastrointest Liver Physiol* **292**, G930–938.

Rodrigues DM, Li AY, Nair DG & Blennerhassett MG (2011). Glial cell line-derived neurotrophic factor is a key neurotrophin in the postnatal enteric nervous system. *Neurogastroenterol Motil* **23**, e44–56.

Saavedra A, Baltazar G, Santos P, Carvalho CM & Duarte EP (2006). Selective injury to dopaminergic neurons up-regulates GDNF in substantia nigra postnatal cell cultures: role of neuron–glia crosstalk. *Neurobiol Dis* **23**, 533–542.

Sanchez MP, Silos-Santiago I, Frisen J, He B, Lira SA & Barbacid M (1996). Renal agenesis and the absence of enteric neurons in mice lacking GDNF. *Nature* **382**, 70–73.

Sarosi GA, Barnhart DC, Turner DJ & Mulholland MW (1998). Capacitative Ca^{2+} entry in enteric glia induced by thapsigargin and extracellular ATP. *Am J Physiol* **275**, G550–555.

Sasselli V, Boesmans W, Vanden Berghe P, Tissir F, Goffinet AM & Pachnis V (2013). Planar cell polarity genes control the connectivity of enteric neurons. *J Clin Invest* **123**, 1763–1772.

Sasselli V, Pachnis V & Burns AJ (2012). The enteric nervous system. *Dev Biol* **366**, 64–73.

Sato Y & Heuckeroth RO (2008). Retinoic acid regulates murine enteric nervous system precursor proliferation, enhances neuronal precursor differentiation, and reduces neurite growth *in vitro*. *Dev Biol* **320**, 185–198.

Schemann M & Neunlist M (2004). The human enteric nervous system. *Neurogastroenterol Motil* **16 Suppl 1**, 55–59.

Uesaka T, Jain S, Yonemura S, Uchiyama Y, Milbrandt J & Enomoto H (2007). Conditional ablation of GFRα1 in

© 2016 The Authors. The Journal of Physiology © 2016 The Physiological Society

postmigratory enteric neurons triggers unconventional neuronal death in the colon and causes a Hirschsprung's disease phenotype. *Development* **134**, 2171–2181.

Uesaka T, Nagashimada M & Enomoto H (2013). GDNF signaling levels control migration and neuronal differentiation of enteric ganglion precursors. *J Neurosci* **33**, 16372–16382.

Van Landeghem L, Chevalier J, Mahe MM, Wedel T, Urvil P, Derkinderen P, Savidge T & Neunlist M (2011). Enteric glia promote intestinal mucosal healing via activation of focal adhesion kinase and release of proEGF. *Am J Physiol Gastrointest Liver Physiol* **300**, G976–987.

von Boyen GB, Steinkamp M, Geerling I, Reinshagen M, Schafer KH, Adler G & Kirsch J (2006). Proinflammatory cytokines induce neurotrophic factor expression in enteric glia: a key to the regulation of epithelial apoptosis in Crohn's disease. *Inflamm Bowel Dis* **12**, 346–354.

Wang H, Hughes I, Planer W, Parsadanian A, Grider JR, Vohra BP, Keller-Peck C & Heuckeroth RO (2010). The timing and location of glial cell line-derived neurotrophic factor expression determine enteric nervous system structure and function. *J Neurosci* **30**, 1523–1538.

Wu JJ, Chen JX, Rothman TP & Gershon MD (1999). Inhibition of *in vitro* enteric neuronal development by endothelin-3: mediation by endothelin B receptors. *Development* **126**, 1161–1173.

Xiao W, Wang W, Chen W, Sun L, Li X, Zhang C & Yang H (2014). GDNF is involved in the barrier-inducing effect of enteric glial cells on intestinal epithelial cells under acute ischemia reperfusion stimulation. *Mol Neurobiol* **50**, 274–289.

Young HM, Bergner AJ & Muller T (2003). Acquisition of neuronal and glial markers by neural crest-derived cells in the mouse intestine. *J Comp Neurol* **456**, 1–11.

Zhang W, Segura BJ, Lin TR, Hu Y & Mulholland MW (2003). Intercellular calcium waves in cultured enteric glia from neonatal guinea pig. *Glia* **42**, 252–262.

Zhou R, Niwa S, Homma N, Takei Y & Hirokawa N (2009). KIF26A is an unconventional kinesin and regulates GDNF-Ret signaling in enteric neuronal development. *Cell* **139**, 802–813.

Additional information

Competing interests

The authors declare no competing financial interests.

Author contributions

All authors contributed to the final version of the manuscript. C.L-B-S., J.C., S.T., E.O., F.C., M.N. and H.B. designed the experiments, analysed and interpreted the data; C.L-B-S., J.C., E.O. and F.C. collected and analysed the data; C.L-B-S., F.C., S.T., M.N. and H.B. revised the article critically for important intellectual content. All authors approved the final version of the manuscript.

Funding

This work was supported by INSERM, the Region Pays de la Loire (Parimad), Fondation LCL and Fondation SantéDige.

Acknowledgements

We are grateful to Tony Durant for help with cell culture.

© 2016 The Authors. The Journal of Physiology © 2016 The Physiological Society